COBEM 2023 27TH INTERNATIONAL CONGRESS OF MECHANICAL ENGINEERING

ABCM Brazilian Society of Mechanical Sciences and Engineering
27th ABCM International Congress of Mechanical Engineering
December 04-08, 2023, Florianópolis-SC, Brazil

COBEM2023-1632
STUDY OF ELECTRICAL ENERGY CONSUMPTION IN MILLING SURFACES UNDER DIFFERENT MACHINING CONDITIONS

Raphael Wildner Xavier
João Carlos Espindola Ferreira
Adriano Fagali de Souza
Federal University of Santa Catarina
raphael.xavier@ufsc.br
j.c.ferreira@ufsc.br
adriano.fagali@ufsc.br

Abstract. *The study of electrical energy consumption during machining is relevant to (a) reducing the electric power consumed by the machine during machining, (b) monitoring tool life, and (c) obtaining the final cost of the produced part. Machining strategies influence the machine's electrical energy consumption and machining time, but few works have been found in the literature that investigated such influence. Given this scenario, the objective of this work was to evaluate the influence of machining strategies, the cutting speed, depths of cut, and feed parameters on the electrical energy consumption in milling AISI P20 steel parts with different part geometries. Initially, the acquisition of electric power in roughing was investigated, machining in 2.5D with different cutting parameters. Subsequently, the electric power consumption and the mean roughness R_a were obtained in finish milling the mold of a connecting rod using the following strategies generated by the NX software: zigzag, contour parallel, zig, and concentric zigzag. A carbide ball-end mill was used for finishing, and the influence of tool wear was also investigated. Then, the electric power consumption was examined in milling a complex surface using a G-code numerical control (NC) program generated by the NX software and a modified G-code program. Non-cutting machining tests were also carried out to obtain the electrical energy generated by other devices present in the machine. The tests were performed using a 4-axis Romi D 600 CNC milling machine. A signal conditioner was used to measure the power and electrical energy consumed in the spindle, and a system available in the CNC Fanuc called "S1 load" that measures the load in relation to the spindle speed. The machining strategy with the lowest energy consumption was the contour parallel. Several peaks of electric power consumption occurred in the concentric zigzag strategy, and bands with more significant variation in electric power at the end of the G-code program. The zig and zigzag strategies had electric power peaks at the beginning of the G-code programs. The zigzag strategy resulted in the lowest mean roughness among the studied strategies. Using the modified G-code program led to higher electric power consumption during finish milling but reduced machining time.*

Keywords: *Milling Strategies, Electrical Energy Consumption, Machining, Sustainable Manufacturing*

1. INTRODUCTION

There are many tool shops that manufacture injection molds in Brazil and other countries. According to De Souza et al. (2019), several products containing complex surfaces can currently be found on the market: electronic products, home appliances, the automotive industry, the medical industry, and toys, among others.

Milling is a process commonly used in manufacturing injection molds, and milling tool paths are constantly studied in engineering. Ochoa González and Ferreira (2019) studied different tool paths for rough milling 2.5D pockets. The axial depth of cut remains constant when milling in 2.5D (Gupta et al., 2005). Liu et al. (2016) pointed out that, in milling, the tool path and the cutting parameters are important because they influence the machining time, the machine's electrical energy consumption, and tool wear. Solheid et al. (2017) evaluated the energy consumption during milling 2.5D pockets in AISI P20 steel using different tool paths and suggested optimizing the cutting parameters to reduce electrical energy consumption. Amaral and Ferreira (2017) investigated hardened steel milling and suggested applying different milling strategies in different part geometries. Santos et al. (2020) investigated energy consumption in milling as a function of tool path variation and machining parameters in AISI P20 steel and suggested evaluating the influence of different cutting tool geometries on energy consumption. De Souza et al. (2019) studied the influence of machining strategies generated by different CAM software on surface quality and machining time.

Kurukulasuriya et al. (2018), Hong et al. (2017), and Budinoff et al. (2016) highlighted the importance of reducing the consumption of electrical energy by machine tools. Bhise and Jogi (2021) and Vardhan et al. (2017) studied the effect of different cutting parameters on electrical energy consumption during milling AISI P20 steel. Milan et al. (2021) compared the machinability of the calcium-treated mold steel (AISI P20 UF) with the non-treated AISI P20 through slot milling tests using triple-coated cemented carbide tools, and power consumption was one of the outputs they obtained.

Machining strategies influence the machine's electrical energy consumption and machining time, but few works have been found in the literature that investigated such influence for different part geometries. Thus, the objective of this work was to evaluate the influence of machining strategies, the cutting speed, depths of cut, and feed parameters on the electrical energy consumption in milling AISI P20 steel parts with different part geometries. Initially, the acquisition of electric power in roughing was investigated, machining in 2.5D with different cutting parameters. Subsequently, the electric power consumption and the mean roughness R_a were obtained in finish milling the mold of a connecting rod using the following strategies generated by the NX software: zigzag, contour parallel, zig, and concentric zigzag. A carbide ball-end mill was used for finishing, and the influence of tool wear was also investigated. Then, the electric power consumption was examined in milling a complex surface using a G-code numerical control (NC) program generated by the NX software and a modified G-code program. Non-cutting machining tests were also carried out to obtain the electrical energy generated by other devices present in the machine.

2. MATERIALS AND METHODS

The parts were machined on a 4-axis ROMI D 600 milling machine with a CNC Fanuc 0iMC, with a power of 30 kW. A signal conditioner was used to measure the power and electrical energy consumed in the spindle, and a system available in the CNC Fanuc called “S1 load” that measures the load in relation to the spindle speed. The machine tool can be programmed to notify the operator when the S1 load value reaches a predefined limit during machining, at which the operator can interrupt machining and check the tool conditions. If the wear is significant, the operator changes the tool.

For the different machining strategies, the cutting parameters were changed in roughing and finishing, obtaining different values of electrical energy consumption. In this way, the machining strategy with the lowest electricity consumption is identified, and the path that leads to a reduced mean roughness (R_a) of the machined parts.

NX software (version 9) was used to generate the cutting parameters for rough and finish milling surfaces. The cutting parameters were used to compare the electrical energy consumption by the machine with the cutting parameters generated by the software CAMSpeed (Käsemodel et al., 2019).

The CAMSpeed software changes the G-code generated by CAM software, inserting commands to modify the spindle speed and feed rate at the end of each block when necessary. When machining complex surfaces, the cutting speed is not constant when using the ball-end milling tool because the contact radius between the tool and the part's surface varies depending on the part's geometry. Thus, the CAMSpeed software compensates for this variation in the contact radius, increasing the spindle speed.

Initially, a study was carried out to verify the sensitivity of the data acquisition system. Linear passes were performed at different cutting depths (0.5 mm, 1.0 mm, 2.0 mm, 3.0 mm) and cutting speeds (104 m/min, 260 m/min, 408 m/min) to machine an AISI P20 steel part. An end mill with two carbide cutting inserts was used.

Subsequently, a study was carried out to determine the electrical energy consumed as a result of the finish machining strategies. An AISI P20 steel mold of a connecting rod was machined (Figure 1) using the following strategies generated by the NX software: zigzag, contour parallel, zig, and concentric zigzag. A carbide ball-end mill was used for finish machining, with a 6 mm diameter, 50 mm length, and two cutting edges.

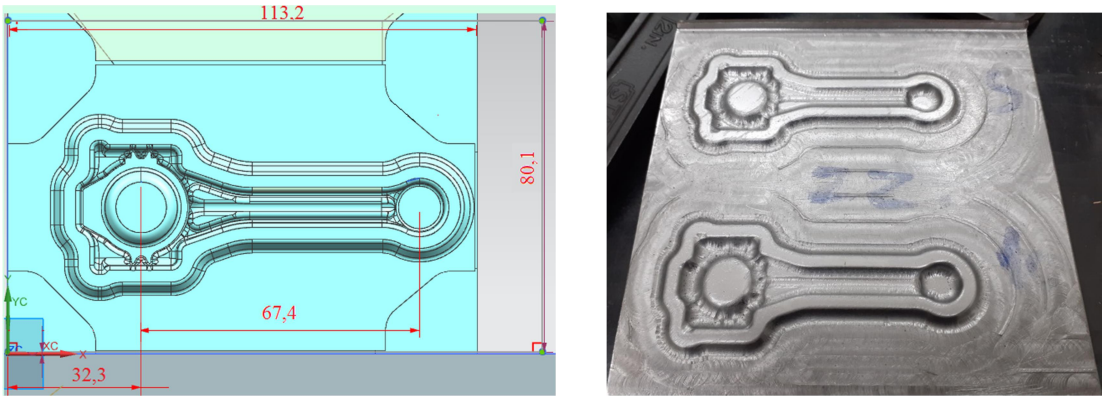

Figure 1. Top view of a connecting rod’s CAD drawing (left), and the machined part using different strategies (right)

Then, the surface on the AISI P20 steel part in Figure 2 was machined using tool paths generated by the NX software, as well as by the G-code modified by the CAMSpeed software. The initial cutting parameters for both programs are spindle speed = 3980 rpm, and feed = 796 mm/min. A 16 mm diameter ball-end mill with coated carbide inserts was used.

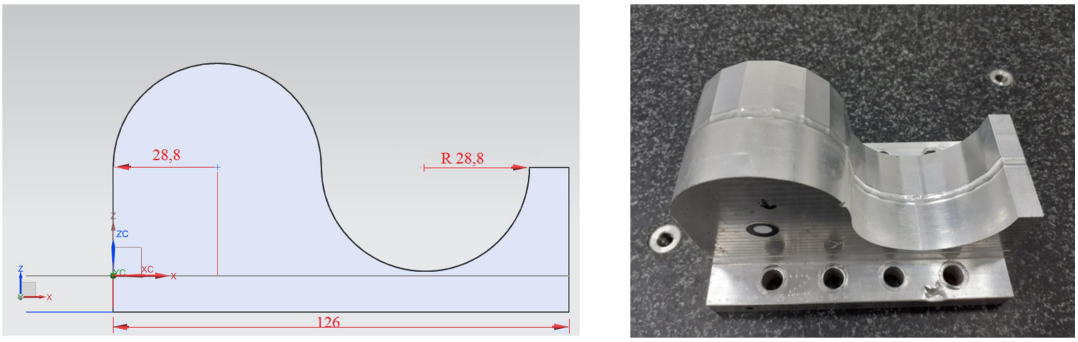

Figure 2. Side view of a CAD drawing of the part with a complex surface (left), and the corresponding machined part (right)

3. RESULTS AND DISCUSSION

3.1. Power measurement without removing material

In order to determine the electric power and verify the functioning of the measuring equipment at different spindle speeds, tests were carried out with the spindle rotating without load. The electrical voltage of the spindle motor was assumed to be constant. The electric power consumption was obtained for each speed range in a time interval of 7 seconds, building the electric power curves as a function of the spindle speed. Phase voltage was equal to 380 V, and motor efficiency was equal to 0.85%.

It was observed the occurrence of an electric power peak of 6500 W when the spindle motor is turned on and, after this peak, the motor stabilizes for each speed range. The spindle speed that consumed the most power corresponded to 1600 rpm.

Figure 3 shows the curves for electric power in watts (in blue) and load in percentage (in red) for different spindle speeds (without removing material) in a steady state. One of the causes for the larger power consumption at lower spindle speeds is that the electric motor's torque is initially large, and, for higher spindle speeds, the torque decreases, leading to a reduction in power. Also, it is observed that, for values above approximately 4900 rpm, there was an increase in power and load that may have been caused by losses such as friction, which may lead to heat (Denkena et al., 2020).

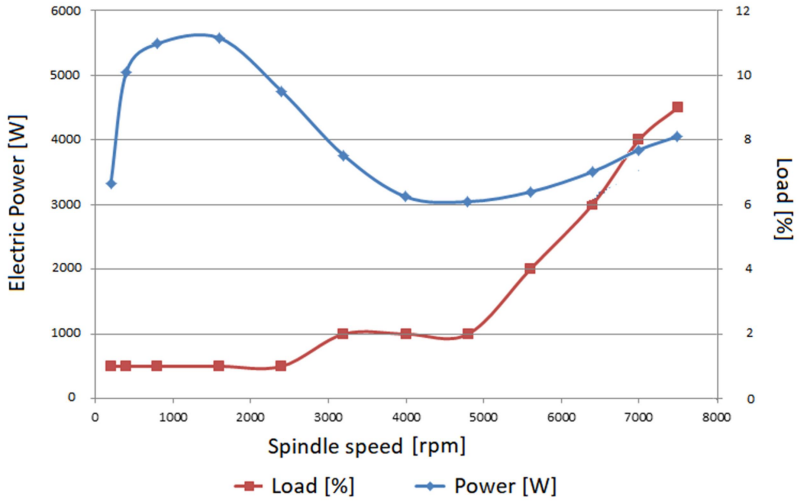

Figure 3. Power and load curves as a function of spindle speed without material removal

3.2. Measuring power in different finishing strategies

For measuring power in different milling strategies, four strategies available in the NX software were used: zig, concentric zigzag, contour parallel, and zigzag (Figure 4). The following cutting parameters were used: cutting speed V_c = 120 m/min, s = 6366 rpm, feed speed V_f = 1900 mm/min, feed per tooth f_z = 0.15 mm/tooth, axial depth of cut a_p = 0.5 mm, radial depth of cut a_e = 0.1 mm. A new tool was used for the finish machining, and then the tool was changed every two runs to eliminate the influence of wear.

The values of average electric power obtained were: Zig = 3371 W, concentric zigzag = 3379 W, contour parallel = 3238 W, zigzag = 3346 W. It can be seen that the values are practically equal.

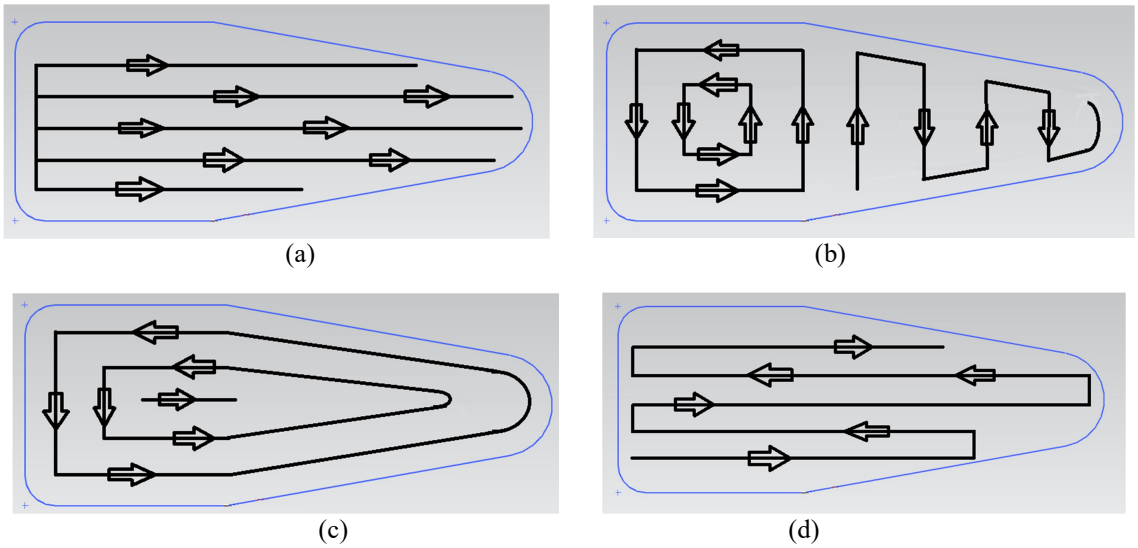

Figure 4. Top view of tool path strategies to machine the region represented in blue color: (a) zig; (b) concentric zigzag; (c) contour parallel; (d) zigzag

In order to determine the mean roughness R_a, nine roughness measurements were made in the direction perpendicular to the grooves on the surface with a bench roughness meter. Three measurements were made on the circle and three measurements on each side of the connecting rod. The values obtained for the mean roughness were: zig = 1.6 µm; concentric zigzag = 2.7 µm; contour parallel = 1.9 µm; zigzag = 1.2 µm. It is observed that the highest mean roughness was obtained in the concentric zigzag strategy, equal to 2.7µm.

In the case of large batches of parts, it is important to identify the strategy that consumes the least energy. Table 1 shows the strategies with their respective finish milling times and energy consumption. It is observed that the zig strategy consumed the most energy, which was 65% more than the contour parallel strategy. The concentric zigzag strategy came second, consuming 32% more energy than the contour parallel strategy. The contour parallel strategy was the strategy that consumed less energy. Finally, the zigzag strategy was the third strategy that consumed the most energy, 10% more electricity than the contour parallel strategy.

Table 1. Time and energy consumed using different milling strategies

Milling Strategies	Time [h]	Energy [kWh]
Zig	0.4755	1.603
Concentric zigzag	0.37944	1.282
Contour parallel	0.29972	0.970
Zigzag	0.32	1.071

Subsequently, finish milling was carried out using the zigzag strategy with the presence of tool wear. The cutting parameters were: V_c = 120 m/min, f_z = 0.15 mm/tooth, a_p = 0.5 mm. Using the images obtained using the optical microscope, the flank wear (VB) of the tool used was equal to 0.18 mm.

The values of mean roughness R_a for the zigzag strategy using tools without and with wear were equal to 1.2 µm and 3.2 µm, respectively.

3.3. Measuring electric power in roughing with new and worn cutting tools

The electric power was obtained using an end mill with a 20 mm diameter with two coated carbide inserts. The following parameters were used in the first test: cutting speed V_c = 104 m/min, spindle speed = 1653 rpm, feed speed V_f = 400 mm/min, feed per tooth f_z = 0.121 mm/tooth, radial depth of cut a_e = 20 mm. Figure 5(a) shows the electric power curves for the following axial depths of cut a_p: 0.5 mm, 1.0 mm, 2.0 mm and 3.0 mm. Note that the curves are practically in the same range of values, but for a_p equal to 3.0 mm, there is an average power of 5750 W.

Figure 5(b) illustrates the curves obtained for V_c = 260 m/min, s = 4140 rpm, V_f = 1000 mm/min. It is noticed that with the increase in cutting depth there is an increase in the electric power consumption, reaching 6000 W for a_p = 3.0 mm, and there is a distinction between the electric power consumption for each depth of cut compared with the spindle speed of 1653 rpm. Figure 5(c) was obtained for cutting parameters V_c = 408 m/min, s = 6500 rpm, V_f = 1600 mm/min. Note that the rise in spindle speed to 6500 rpm increases electric power consumption for the same cutting depths shown in Figure 5(b), reaching 6300 W for a_p = 3 mm.

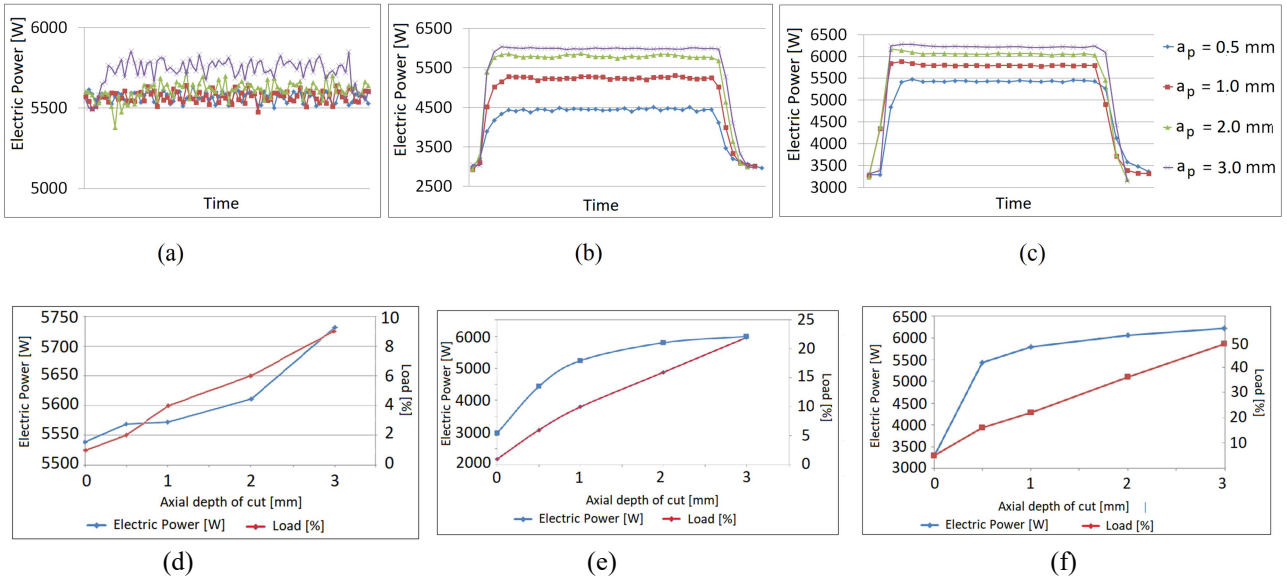

Figure 5. Electric power curves as a function of cutting depth: (a) s=1653 rpm using the electric power sensor; (b) s=4140 rpm using the sensor; (c) s=6500 rpm using the sensor. Electric power and spindle load curves: (d) s=1653 rpm; (e) s=4140 rpm and (f) s=6500 rpm

Figure 5(d) shows a power curve in watts (in blue) and a S1 load curve (on the spindle) in percentage (in red) for a spindle speed of 1653 rpm. Note that the power obtained using the electric power sensor increases as a function of the cutting depth, having a similar behavior to the curve obtained from the S1 load.

Figure 5(e) shows the power and S1 load curves for a spindle speed of 4140 rpm. Note that with the increase in the cutting depths, there is an increase in the electric power using the sensor and the S1 load. Figure 5(f) shows the S1 load and power curves for a spindle speed of 6500 rpm. It is observed that, similarly to the result shown in Figure 5(e), the load curve has a linear behavior.

Subsequently, roughing tests were carried out to determine changes in energy consumption using cutting tools with wear. A tool with a diameter of 20 mm with two cutting edges was used, with a flank wear VB = 0.5 mm.

Figure 6 shows graphs of electric power as a function of different cutting depths for parameters V_f = 400 mm/min and f_z = 0.121 mm/tooth. Milling was carried out with a_p = 0.5 mm and 1.0 mm in order to preserve the tool because, at higher depths, with tool wear, inappropriate chips were formed.

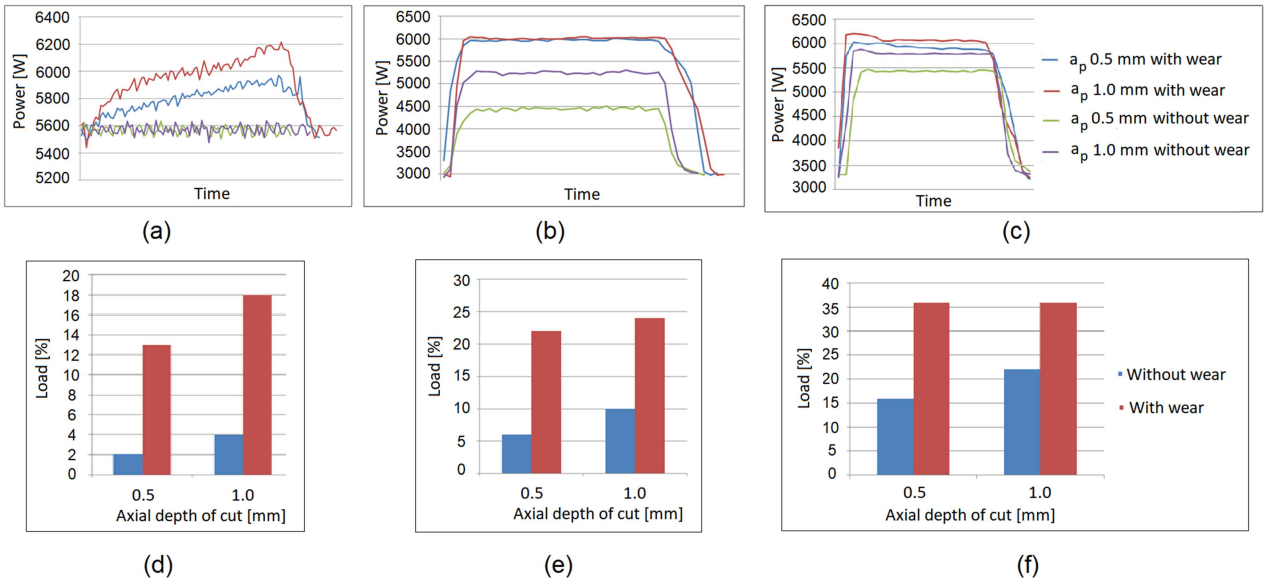

Figure 6. Electric power curves and S1 load for a_p = 0.5 and 1.0mm, with and without tool wear. Spindle speeds: (a) 1653 rpm, (b) 4140 rpm, (c) 6500 rpm, (d) 1653 rpm, (e) 4140 rpm, and (f) 6500 rpm

It is observed in Figure 6(a) that, for new cutting tools, the influence of cutting depths was not perceptible to the power signals. However, the S1 load values in Figure 6(d) indicate sensitivity to different cutting depths at 1653 rpm. In Figures 6(b) and 6(e) (spindle speed = 4140 rpm), both the power signal and the S1 load detected the different a_p values when using the new tool. Although the power increased with worn tools compared with new tools, the different cutting depths were not detected, whereas the S1 load in Figure 6(e) detected different depths of cut and tool wear. For a spindle speed of 6500 rpm, the values of power in Figure 6(c) show that the different cutting depths for new and worn tools were detected, and the S1 load in Figure 6(f) for new tools. However, the S1 load in Figure 6(f) did not detect the different depths of cut for worn tools with spindle speed = 6500 rpm.

3.4. Measuring power for tool paths generated using NX and CAMSpeed for a part with complex geometry

The NX software was used to generate the G-code, and CAMSpeed software was used to modify the G-code. The initial cutting parameters were: s = 3980 rpm, V_f = 796 mm/min. Figure 7 shows the side view of the part and the tool path for finish milling using a ball-end mill tool (in light blue).

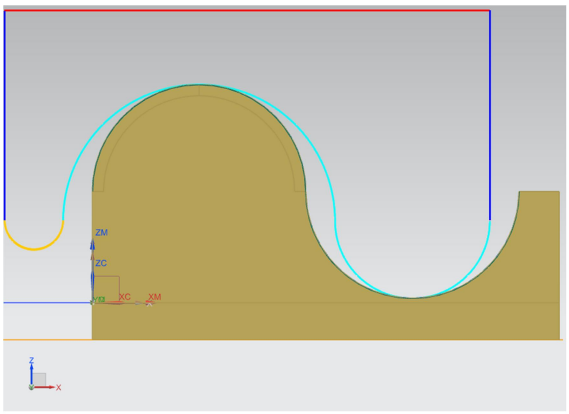

Figure 7. Side view of the part with a complex surface, and the tool path for finishing using a ball-end milling tool

Figure 8 shows the tool path and the spindle speed curve, the feed curve, and the consumed electric power. It is observed that the spindle speed and feed curves have similar behavior. When the tool is in the ascending portion of the first movement stage, there is a gradual increase in the spindle speed, as well as a gradual increase in the feed speed up to a spindle speed of 7500 rpm and a feed speed of 1500 mm/min. After this stage, the tool is at the top of the complex surface and, at that moment, the consumed power is equal to 3700 W, and the tool starts to move downwards, with a gradual decrease in the spindle speed and a reduction in the feed speed until s = 4131 rpm and V_f = 826 mm/min. At that moment, the tool has a maximum contact radius between the part and the tool, equal to 3 mm. Then, the tool continues its movement downwards to the lowest point of the concave surface, and, at that moment, the spindle speed is equal to 7500 rpm, and the feed speed is equal to 1500 mm/min. Finally, the tool traverses the last concave path upwards, gradually reducing spindle speed and feed speed up to s = 4131 rpm and V_f = 826 mm/min.

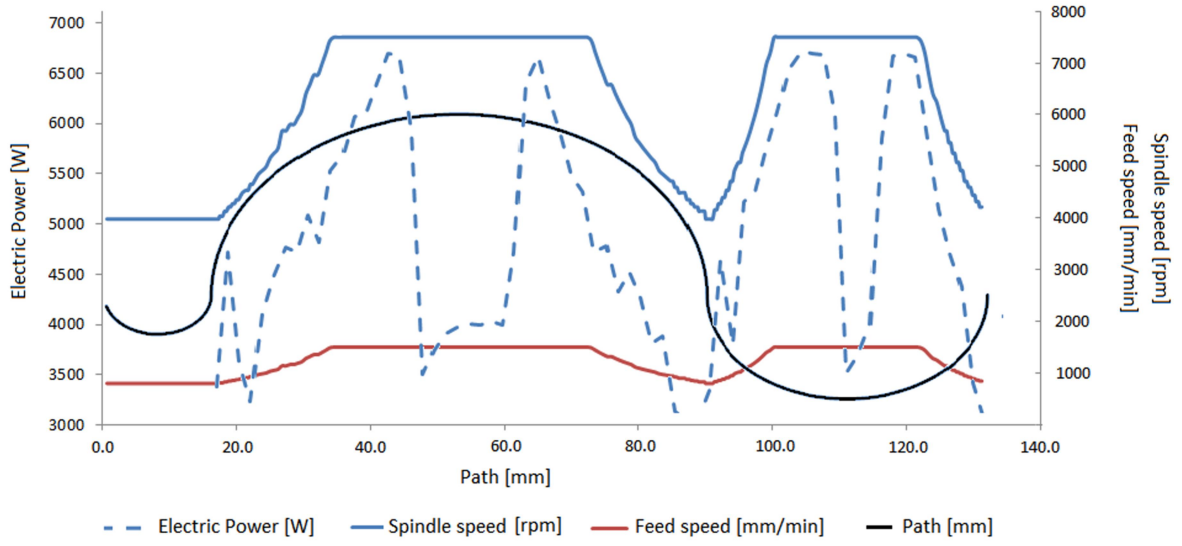

Figure 8. Curves for power [W], spindle speed s [rpm], feed speed V_f [mm/min], and tool path [mm]

For plotting Figure 8, the average of the values of electric power obtained in the first 11 passes in finish milling was calculated using the CAMSpeed software. It is observed that the consumption of electric power varies at the beginning of milling, with a peak of 4700 W. Then, there is a reduction in power consumption to about 3300 W, and, at this moment, the tool begins to reduce its contact radius. When the tool is contouring the convex surface, there is a progressive increase in consumption up to about 6700 W, and, at this value, the tool reaches the top of the convex surface with a contact radius close to zero. Near the top of the convex surface, when the motor increases the spindle speed to 7500 rpm, there is a reduction in electric power consumption, reaching a value of 3500 W.

After reaching the top, the tool starts to descend along the convex surface and, consequently, the power consumption increases, reaching another power peak equal to 6600 W, progressively decreasing until the value of about 3300 W. At this value, the tool almost has the full contact radius to the surface. When the tool is at full contact radius, there is a small power peak of 4500 W. Then, the motor progressively increases power consumption until it reaches 6600 W, when the tool is at a contact radius close to zero on the concave surface. When the tool is at zero contact radius, there is a sudden drop in electric power consumption, reaching 3300 W, and then, there is a rapid increase in consumption up to 6600 W again. When the tool contact radius starts to increase, there is a reduction in electric power consumption to approximately 3300 W.

Figure 9 shows the electric power resulting from the execution of the G-code program used for a finishing pass. Note that, in the curve using the CAMSpeed software, there are four peaks of electric power reaching approximately 6500 W.

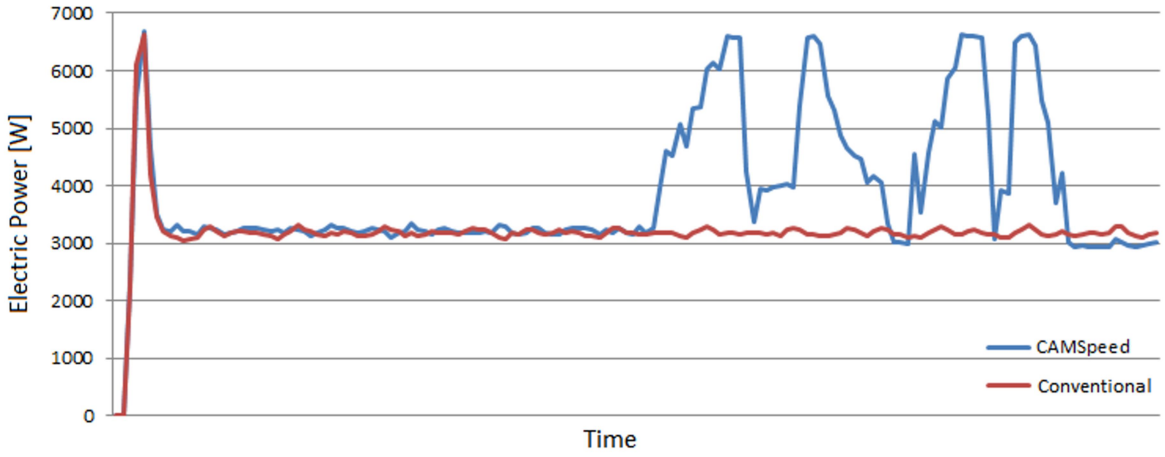

Figure 9. Curves of the electric power for the tool paths generated by executing G-code programs using the conventional (only NX) and CAMSpeed software

Table 2 shows the electric power, standard deviation, load and time depending on the program used. Using the CAMSpeed software, it is observed that the load varies between 2% and 150% in the case of no material removal. It is also noticed that there was a 38% increase in electric power consumption using the CAMSpeed software, and the time was reduced by approximately 18%. The program using the CAMSpeed software had electrical energy consumption approximately 13% higher than the conventional program (i.e. using only NX).

Table 2. Electric power, standard deviation, load, time, and energy depending on the programs used when no material is removed

Program	Electric Power [W]	Standard Deviation	Load [%]	Time	Energy [kWh]
CAMSpeed	4398	1326	2 - 150	11min 33secs	0.8466
Conventional	3184	124	2	14min 8secs	0.750

In order to obtain the electric power when machining in a contour parallel tool path of a complex surface, a 16 mm diameter ball-end mill was used. Figure 10 shows the electric power obtained by the signal acquisition system during machining. It can be noticed that, for a spindle speed of 1653 rpm, there is a consumption of approximately 5500 W of electric power, and the same consumption occurs using the CAMSpeed software. For a spindle speed of 4140 rpm, there is a consumption of 3000 W of electric power; for a spindle speed of 6500 rpm, there is a consumption of 3500 W. It can be noticed that only for the spindle speed of 1653 rpm there was an effective difference in average consumption between machining and not machining.

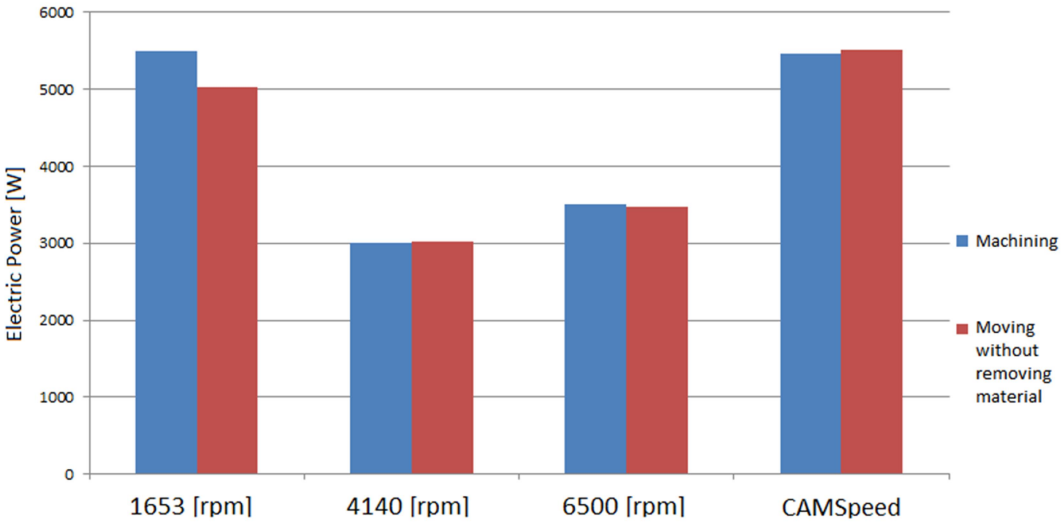

Figure 10. Electric power as a function of spindle speed when removing or not removing material from a complex surface

It is observed in Figure 10 that higher values of electric power were obtained for the spindle speed of 1653 rpm compared with the speed of 4140 rpm. This may have been because the lower the spindle speed, the higher the chip load (i.e., chip thickness removed by each tooth in a revolution) for a specific value of feed speed V_f, which increases cutting resistance (Wang et al., 2019). In case the material is not removed, there is no cutting resistance; thus, increasing the spindle speed will not significantly affect power consumption (Wang et al., 2019).

In the case of using a worn tool, Figure 11 shows the cutting edge with flank wear VB = 0.5 mm, and crater wear (left) and the tool without wear (right).

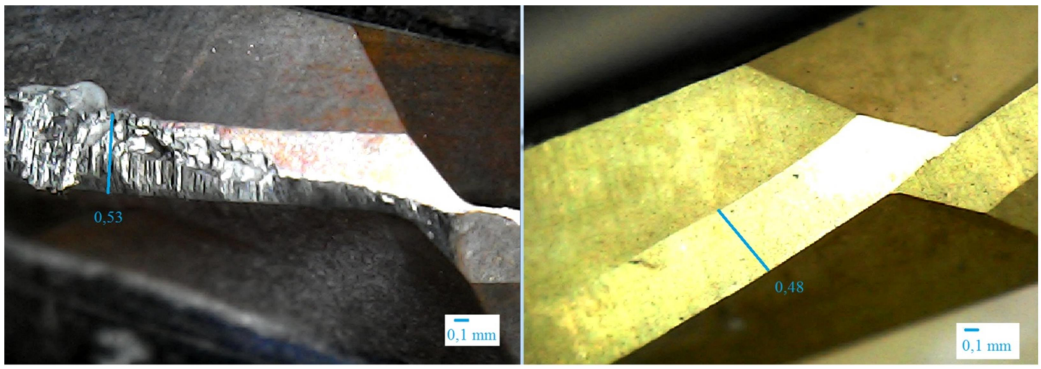

Figure 11. Cutting edge with flank and crater wear (left), and cutting edge without wear (right)

Table 3 shows the average consumed power for the different spindle speeds. In these tests, the following parameters were used: a_p = 0.2 mm, f_z = 0.1 mm/tooth, tool diameter = 16 mm.

Table 3. Average electric power as a function of spindle speed

Spindle Speed [rpm]	Average Electric Power [W]
1653	5577
4140	2890
6500	3674
CAMSpeed	5488

Figure 12 shows the values obtained for average electric power. It is observed that the power acquisition system cannot distinguish machining with and without the presence of tool wear (Hsieh et al., 2012), nor distinguish whether the tool is moving with or without material removal when finishing (Quintana et al., 2011).

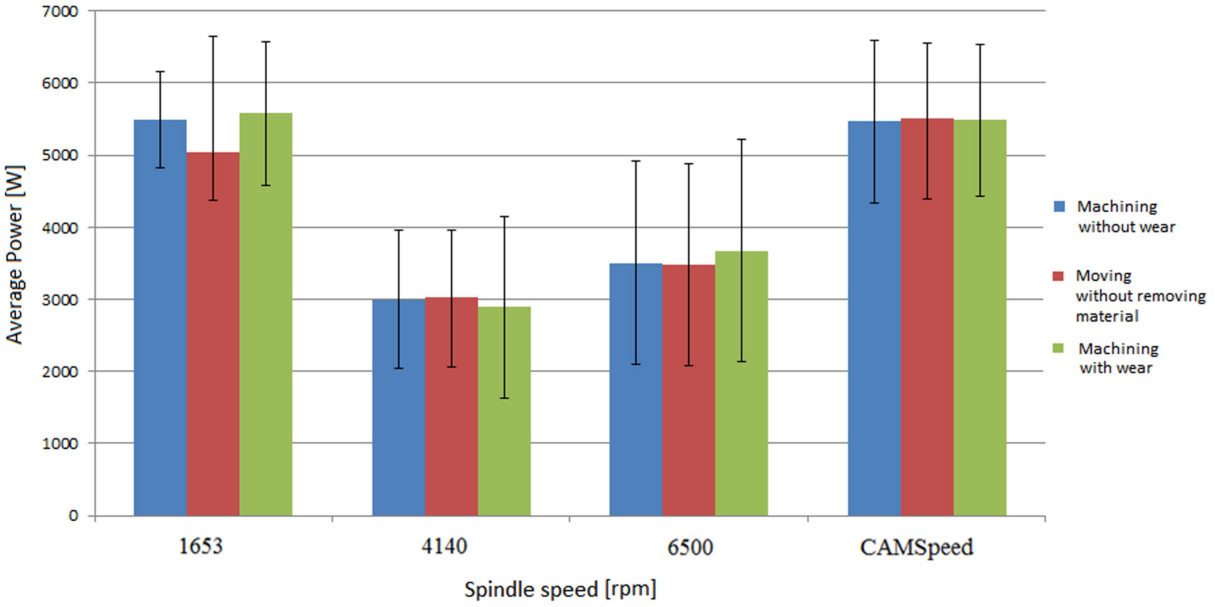

Figure 12. Values of average electric power obtained using a system monitoring the machining of a complex surface with a ball-end milling tool: machining with a new tool, no material removal, and worn tool

4. CONCLUSIONS AND FUTURE WORK

Regarding finish milling the connecting rod using different machining strategies, the electric power consumption without material removal was approximately equal in all strategies considered. During finish machining, electric power consumption was lower in the contour parallel strategy, and, in this same strategy, the average electrical energy consumption was the same without removing material and in finish machining.

In the concentric zigzag strategy, several peaks of electric power consumption occurred, as well as bands with more significant variation in electric power at the end of the G-code program. The zig and zigzag strategies had electric power peaks at the beginning of the G-code programs. The strategy that consumed less electric power was the contour parallel strategy, in which, at the beginning of the program, there was a peak of approximately 4100 W and, after this peak, the power consumption remained constant, with more variation in electric power occurring at the end of the G-code program, with three peaks of electric power above 4000 W, and more peaks above 3500 W at the end of the program. In terms of mean roughness, the zigzag strategy resulted in the lowest mean roughness among the studied strategies.

The cost of electrical energy for a batch of parts similar to the geometry of the connecting rod studied, produced through the contour parallel strategy, can lead to a reduction of 65% in electrical energy compared with the zig strategy. This value can be significant in tool shop manufacturing or a factory operating on a batch manufacturing basis.

It was observed that the electric power acquisition system does not recognize the wear on the edge of the cutting insert. Also, the S1 load on the CNC Fanuc does not distinguish the presence of tool wear when finish milling.

Regarding finish milling the part with complex geometry using the G-code program generated by the NX software (conventional) and the program modified by the CAMSpeed software, a shorter machining time was obtained using the CAMSpeed software, but there was a higher consumption of electric power. The electric power consumption decreased when the tool moved along the complex surface in the region where the tool contact radius is zero.

Similarly to the machining of the mold for the connecting rod mentioned previously, it was observed that the electric power monitoring system does not distinguish the presence of wear on the cutting tool edge when finishing the complex surface. The obtained S1 loads also indicate the lack of sensitivity to detect wear on the cutting tool.

It is suggested in future works to carry out milling operations with other values of the parameters cutting speed, feed, and depths of cut. It is also suggested to measure the cutting forces, mainly during roughing.

5. REFERENCES

Amaral, G.F.; Ferreira, J.C.E. 2017. *Evaluation of hardened steel milling considering economic, social and environmental aspects*. In: 9th Brazilian Congress of Manufacturing Engineering (COBEF), Joinville, Brazil. ABCM (in Portuguese).

Bhise, V.Y.; Jogi, B.F. 2021. *Experimental investigation and theoretical modelling of P20 steel by using CNC end milling machining process*. In: Journal of Physics: Conference Series (Vol. 1854, No. 1, p. 012011). IOP Publishing.

Budinoff, H.; Bhinge, R.; Dornfeld, D. 2016. *A material-general energy prediction model for milling machine tools*. In: International Symposium on Flexible Automation (ISFA) (p. 161-164). IEEE.

De Souza A. F.; Käsemodel R. B.; Arias M.; Marin F.; Rodrigues A. R. 2019. *Study of tool paths calculated by different commercial CAM systems and influences on the real machining time and surface roughness for milling free-form geometries*. Journal of the Brazilian Society of Mechanical Sciences and Engineering. Vol. 41, No. 9, p. 1-2.

Denkena, B.; Bergmann, B.; Klemme, H. 2020. *Cooling of motor spindles - a review*. International Journal of Advanced Manufacturing Technology, 110, p. 3273-3294.

Gupta, S.K.; Saini, S.K.; Spranklin, B.W.; Yao, Z. 2005. *Geometric algorithms for computing cutter engagement functions in 2.5 D milling operations*. Computer-Aided Design, Vol. 37, No. 14, p. 1469-1480.

Hong, H.; Zhang, C.; Meng, L.; Tian, G.; Yu, J. 2017. *Characterising energy efficiency in maching processes: A milling case*. In: International Conference on Advanced Mechatronic Systems (ICAMechS) (p. 83-88). IEEE.

Hsieh, W.H.; Lu, M.C.; Chiou, S.J. 2012. *Application of backpropagation neural network for spindle vibration-based tool wear monitoring in micro-milling*. International Journal of Advanced Manufacturing Technology, Vol. 61, p. 53-61.

Käsemodel R. B.; Voigt, R.; Marin, F.; De Souza, A. F. 2019. *Study of the milling time of complex shapes keeping constant cutting speed and feed per edge*. In: 10th Brazilian Congress of Manufacturing Engineering (COBEF), São Carlos, SP, Brazil. ABCM (in Portuguese).

Kurukulasuriya, M.; Gamage, J.; Mangala, J. 2018. *A review on the impact of process energy on the environmental performance of milling*. In: International Conference on Production and Operations Management Society (POMS) (p. 1-6). IEEE.

Liu, Z.Y.; Sealy, M.P.; Guo, Y.B.; Liu, Z.Q. 2016. *Real-time monitoring and prognosis of energy consumption in hard milling*. In: 2016 International Symposium on Flexible Automation (ISFA) (p. 422-427). IEEE.

Milan, J.C.; Machado, A.R.; Tomaz, Í.V.; da Silva, L.R.; Barbosa, C.A.; Mia, M.; Pimenov, D.Y. 2021. *Effects of calcium-treatment of a plastic injection mold steel on the tool wear and power consumption in slot milling*. Journal of Materials Research and Technology, Vol. 13, p. 1103-1114.

Ochoa González, D.M.; Ferreira, J.C.E. 2019. *Use of a virtual milling system to generate power-aware tool paths for 2.5-dimensional pocket machining*. Proceedings of the Institution of Mechanical Engineers, Part B: Journal of Engineering Manufacture, Vol. 233, No. 13, p. 2419-2435.

Quintana, G.; Ciurana, J.; Ribatallada, J. 2011. *Modelling power consumption in ball-end milling operations.* Materials and Manufacturing Processes, Vol. 26, No. 5, p. 746-756.

Santos, R.C.; Pereira, M.; Ferreira, J.C.E. 2020. *Energy consumption in milling as a result of different machining parameters and tool paths*. In: IEEE Annual Green Technologies Conference (GreenTech 2020), Oklahoma City, USA, p. 206-211.

Solheid, J.S.; Ferreira, J.C.E.; González, D.M.O. 2017. *Evaluation of energy consumption in the milling process of 2½D pockets for different types of paths*. In: 9th Brazilian Congress of Manufacturing Engineering (COBEF), Joinville, Brazil. ABCM (in Portuguese).

Vardhan, M.V.; Sankaraiah, G.; Yohan, M. 2017. *Effect of process parameters on power consumption in machining of P20 steel in CNC milling*. In: International Conference on Energy, Communication, Data Analytics and Soft Computing (ICECDS) (p. 3217-3220). IEEE.

Wang, S.M.; Lee, C.Y.; Gunawan, H.; Yeh, C.C. 2019. *An accuracy-efficiency-power consumption hybrid optimization method for CNC milling process*. Applied Sciences, Vol. 9, No. 7, p. 1495.

6. RESPONSIBILITY NOTICE

The authors are the only responsible for the printed material included in this paper.